POLITECNICO
MILANO 1863

SCUOLA DI INGEGNERIA INDUSTRIALE
E DELL'INFORMAZIONE

Executive Summary of the Thesis

Ultrafast Terahertz Spectroscopy of Trilayer MoS_2

Laurea Magistrale in Engineering Physics - Ingegneria Fisica

Author: Federico Grandi

Advisor: Prof. Salvatore Stagira

Co-advisors: Eugenio Cinquanta, Caterina Vozzi

Academic year: 2021-2022

1. Introduction

Since the discovery of graphene, the interest in low-dimensional materials has grown considerably. Transition metal dichalcogenides (TMDs) stood out in this category thanks to their peculiar properties arising from their topological structure. In particular, the low dimensionality introduces quantum confinement of the charges that together with the reduced screening of Coulomb forces, results in a higher exciton binding energy. Together with that, the band-gap properties of these materials change drastically when moving from a few to a monolayer configuration, resulting in a shift from an indirect band-gap to a direct one. Of all TMDs, MoS_2 is probably one of the most studied, both in its mono-layer and multi-layer configuration for the potentiality of applying it in several fields of electronics and optics. Zhao et al. in [1] demonstrated and later observed, via Raman spectroscopy, the presence of low-energy vibrational modes arising from the relative motion of the layers in a multi-layer structure of MoS_2 with resonances in the THz region, and also that electron-phonon scattering is the main limiting factor for carriers' mobility. Pizzi et al. [2] provided a tool to mathematically evaluate the position and optical activity of these modes, which have been found to lay all under the 1.75 THz threshold for breathing modes and under 1 THz for shear modes. Given the lack of works regarding the observation of those modes with THz spectroscopy, we will try to identify shear and breathing modes in a trilayer sample of MoS_2 , testing also their interaction with the charge carriers arising from the photoexcitation of the sample.

2. Experimental Setup

The experiments presented in this summary were performed with an ultrafast THz spectroscopy setup. The driving laser is an amplified Ti:Sa laser system, that generates pulses of roughly 25 fs with a repetition rate of 1 kHz at around 790 nm. THz generation is performed via optical rectification in a 1 mm-thick ZnTe crystal with <110> orientation, allowing to achieve bandwidth spanning roughly between 0.5 THz and 2.5 THz. The interaction site where the sample and the laser pulses interact is located in a sealed chamber, fluxed with nitrogen gas during all the experimental acquisition, as water in the atmosphere introduces unwanted absorptions in the THz region. To perform pump-probe experiments a pump line is able to deliver 400 nm pulses with tunable flu-

ence. Detection is performed via electro-optic sampling on a ZnTe crystal allowing for a full reconstruction of the THz field both in amplitude and phase.
The sample is a 2x2 cm substrate of fused silica on top of which the MoS_2 is deposited. The deposition technique exploited liquid-exfoliation to produce trilayer flakes of MoS_2 which were then deposited in three different instances, with the results of obtaining a distribution of flakes centered around the trilayer.

3. Experimental Results

3.1. Static measure

Static measures allow the analysis of the relaxed sample by recording the electric THz field that interacts with it. By performing an acquisition with and without the sample is possible to retrieve the experimental transmission as a function of the pulse frequency, from which is then possible to retrieve the complex refractive index of the specific material.

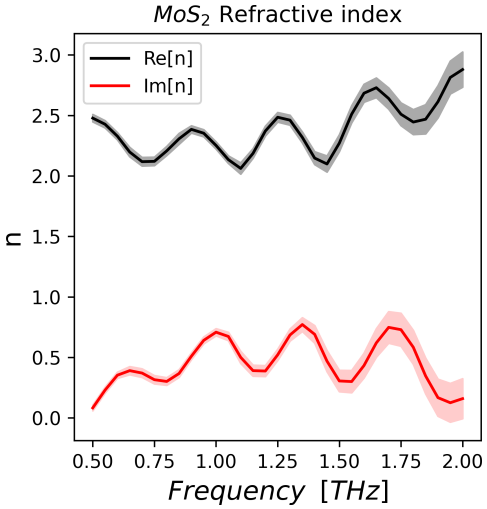

Figure 1: Complex refractive index of MoS_2 . With real part in black and extinction coefficient in red. Shaded regions represents the error bars on the data

The refractive index of MoS_2 , shown in figure 1, was obtained by running an optimization algorithm to fit the experimental transmission with the ideal transmission function derived by evaluating the path traveled by light inside the medium and described in equation 1.

$$T(\omega) = \frac{E_{samp}(\omega)}{E_{ref}(\omega)} = \frac{t_{am}t_{ms}}{t_{as}} e^{id_m k_0(n_m - n_a)} e^{idLk_0(n_s - n_a)} \quad (1)$$

Where t_{ab} is the Fresnel transmission coefficient between media a and b, d_m is the thickness of the sample, n_x is the refractive index of the medium x (a=air, m=MoS_2 , and s=substrate), and dL is a corrective factor to account for imperfections in the substrate thickness.
Starting from the refractive index is then trivial to obtain the complex conductivity. The aim of this analysis is to determine the presence of the low-energy vibrational modes arising from a relative motion of MoS_2 layers. The description of the resonances induced by these vibrational modes was determined starting from the Lorentz oscillator model which supposes resonances in the form of:

$$\sigma_{DL} = \frac{gf}{i(f_0^2 - f^2) + \Gamma f} \quad (2)$$

Where g is the amplitude, f_0 is the central frequency of the resonance, and Γ is the damping rate.
To fit the complex conductivity previously derived it was necessary to suppose the presence of five different Lorentzian, together with a Drude-Smith term describing the presence of free carriers arising from the light n-doping of MoS_2 [3]. The results of the fit are shown in figure 2.
The first four Lorentzian are compatible with the presence of the low energy modes arising from breathing and shear motion of the layers, while the fifth one, at higher frequencies with respect to the observed spectral region, may be compatible with the presence of a trion. Theoretically, given the polarization direction of the THz pulse and the position of MoS_2 layers, breathing mode should not be excitable, but imperfection in the alignment of the pulse's polarization and the position of the MoS_2 flakes on the sample may still allow for observation of these modes.

3.2. 1D dynamic measure

By performing a pump-probe measure with a fixed interaction with the THz pulse is then possible to observe the relaxation dynamics of the

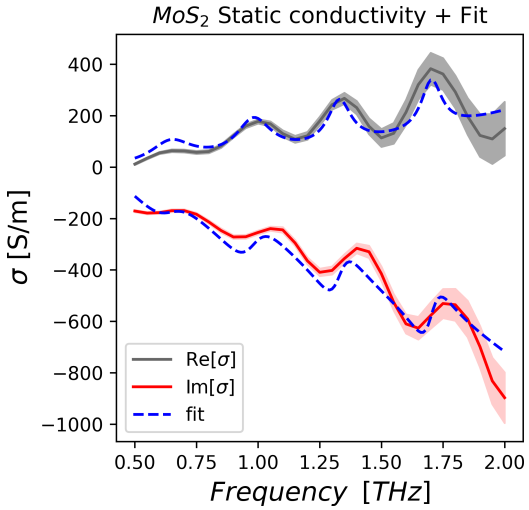

Figure 2: Result of the fit of the complex conductivity of MoS_2 , with the fit represented by blue dashed lines. The shaded area represents the error bars on the data

free charges induced by the pump excitation, together with the possibility of determining information about the mobility of free charges in the sample. It has been shown that the relaxation dynamic in MoS_2 is mainly determined by defect-assisted recombination in the form of Auger and phonon-assisted processes [3]. Observations showed that the decay dynamics could then be divided into two exponential functions with different decay rates.

$$y(t) = A_1 e^{\frac{-t}{\tau_1}} + (1 - A_1) e^{\frac{-t}{\tau_2}} \qquad (3)$$

Following these results, the bi-exponential presented in equation 3 has been applied to fit the normalized relaxation dynamics obtaining the results shown in figure 3.
In particular, we observed a fast recombination rate comparable to the values presented in the literature with $\tau_1 \approx 3\,ps$, while the slower recombination rate resulted in a much faster decay. This effect could be linked to the interaction of the phonon modes with the pump-induced free charges. Considering the confidence intervals of these parameters there is no observation of a fluence dependence and thus the difference between measures could be ascribed to a lower signal-to-noise ratio with a corresponding higher uncertainty on the measure. Regarding the evaluation of carriers' mobility, it is possible to evaluate it considering the absorbance of the sample, given by the manufacturer of the sample itself.

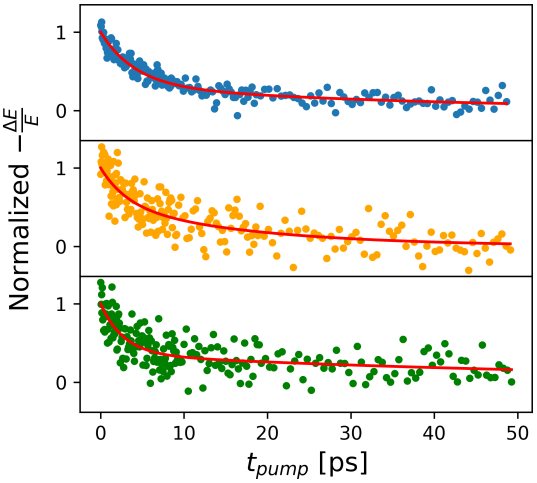

Figure 3: Fit of MoS_2 dynamics at the fluences of: (blue) 95.5 $\mu J\,cm^{-2}$, (orange) 70 $\mu J\,cm^{-2}$, (green) 48.3 $\mu J\,cm^{-2}$

Fluence $[\mu J\,cm^{-2}]$	$\phi\mu$ $[cm^2\,(Vs)^{-1}]$
48.3	5.74
70	4.55
95.5	6.78

Table 1: Carriers' mobility evaluated at three fluences starting from dynamic measurements

The resulting values for carriers' mobility are summarized in table 1. Mobility does not show a clear dependence on fluence and results significantly lower than the value proposed in other works. As defect scattering and electron-phonon coupling seem to be the main limiting factors for charge carriers' mobility, it could be possible that a higher concentration of defect state and the structure of grain boundaries inside the sample determine this reduction in mobility. Moreover, the presence of the phonon resonances observed before could also determine the lower mobility.

3.3. 2D pump-probe measure

To determine the interaction of the previously observed vibrational modes with the presence of free charges induced by a pump pulse it was then necessary to perform a 2D pump-probe experiment. This was a differential measurement between the photoexcited condition and the relaxed one, which allowed the retrieval of the differential transmission induced by the pump pulse. By modeling this term considering the physical model of light transmission in

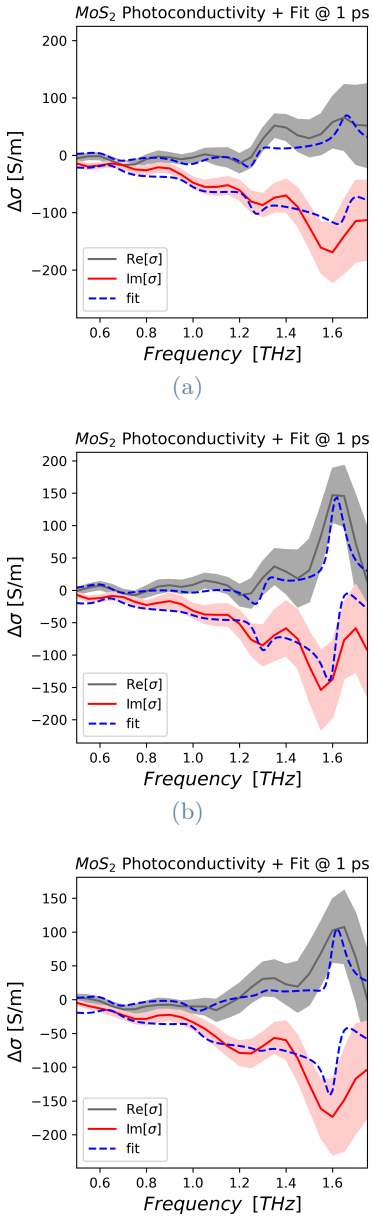

Figure 4: Plot of the differential photoconductivity induced at a fixed $t_{pump} = 1\,ps$ with the evaluated fit at the following fluences: (a) 95.5 $\mu J\,cm^{-2}$, (b) 70 $\mu J\,cm^{-2}$, (c) 48.3 $\mu J\,cm^{-2}$. Error bars are represented with the shaded area

the medium, in equation 4, it is then possible to evaluate the transient change in refractive index and consequentially the differential value of the photoconductivity.

$$T(\omega) = \frac{t_{ap}t_{ps}}{t_{am}t_{ms}} e^{idk_0(n_p - n_m)} \tag{4}$$

Also in this case we observe the presence of some features induced by the pump photoexcitation. The model applied to fit these features is derived from [4] and consists of the differentiation of the Lorentzian of the static fit to account for small changes in amplitude and central frequency:

$$\begin{aligned} d\sigma(f) = &\frac{f}{i(f_0^2 - f^2) + \Gamma f} dg + \\ &+ \frac{-2if_0 gf}{[i(f_0^2 - f^2) + \Gamma f]^2} df_0 \end{aligned} \tag{5}$$

The fit was performed at a pump-probe delay of 1 ps, representing the maximum value of the transient dynamics, for the three different fluences shown in figure 4. The position of the fifth Lorentzian was fixed as we do not expect a shift in the frequency of the trion resonance. The other features undergo some amplitude and central frequency change but there is no clear pattern with respect to the fluence rate. Anyway, the presence of these features can be linked with the coupling between charge carriers and the low-energy vibrational modes, an effect that would also result in a limitation of carriers' mobility.

4. Conclusions

In conclusion, the aim of these experiments was to observe the effects of the low-energy shear and breathing rigid motion of the layers on the photophysical properties of MoS_2. The static measures showed the presence of features in the static conductivity of MoS_2 compatible in their positions with the IR active breathing and shear modes predicted in [2]. The resonances do not perfectly match the expected modes of the trilayer, but this behavior may arise from the uncertainty over the exact layer distribution of the flakes of MoS_2 deposited, which is expected to vary around the trilayer structure. Other than the four observed resonances there is also the fifth feature, out of the observable bandwidth, which could be linked with the presence of a trion resonance. Dynamics measurement determined that the relaxation of excited carriers follows a bi-exponential decay, where the faster decay rate was similar to values reported in the literature [3] and could be linked with the presence of fast defect states in the material, while the slower decay seemed faster with respect to the value reported by other works. This discrepancy could be linked with the coupling of charge carriers with the phonon modes observed with static measures or with an abundance of defect

states in this particular sample. The evaluation of charge mobility seems to confirm these observations as we reported lower mobility with respect to other works. 2D pump-probe measures were then performed to determine the interaction of the low-energy vibrational modes with charge carriers. The resulting change in photoconductivity showed the presence of features that can be linked with the change in amplitude and central frequency of the earlier observed resonances. It is not possible to extrapolate a dependency on fluence as there is not a clearly observable trend in the relative changes of the Lorentzian. Anyway, the presence of these features could be an indicator that the photoexcited charge carriers interact and couple with the phonons inside MoS_2 .

References

[1] Yanyuan Zhao, Xin Luo, Hai Li, Jun Zhang, Paulo T. Araujo, Chee Kwan Gan, Jumiati Wu, Hua Zhang, Su Ying Quek, Mildred S. Dresselhaus, and Qihua Xiong. Interlayer breathing and shear modes in few-trilayer mos2 and wse2. *Nano Letters*, 13:1007–1015, 3 2013.

[2] Giovanni Pizzi, Silvia Milana, Andrea C. Ferrari, Nicola Marzari, and Marco Gibertini. Shear and breathing modes of layered materials. *ACS Nano*, 15:12509–12534, 8 2021.

[3] Haining Wang, Changjian Zhang, and Farhan Rana. Surface recombination limited lifetimes of photoexcited carriers in few-layer transition metal dichalcogenide mos2. *Nano Letters*, 15:8204–8210, 12 2015.

[4] Daming Zhao, Hongwei Hu, Reinhard Haselsberger, Rudolph A. Marcus, Maria-Elisabeth Michel-Beyerle, Yeng Ming Lam, Jian-Xin Zhu, Chan La o vorakiat, Matthew C. Beard, and Elbert E. M. Chia. Monitoring electron–phonon interactions in lead halide perovskites using time-resolved thz spectroscopy. *ACS Nano*, 13:8826–8835, 8 2019.